European Journal of Radiology 112 (2019) 207–213

Contents lists available at ScienceDirect

European Journal of Radiology

journal homepage: www.elsevier.com/locate/ejrad

Research article

The diagnostic value of 4D MRI at 3T for the localization of parathyroid adenomas

Mesut Ozturk[a,*], Ahmet Veysel Polat[a], Cetin Celenk[a], Muzaffer Elmali[a], Seher Kir[b], Cafer Polat[c]

[a] Department of Radiology, Faculty of Medicine, Ondokuz Mayis University, Samsun, Turkey
[b] Department of Internal Medicine, Faculty of Medicine, Ondokuz Mayis University, Samsun, Turkey
[c] Department of General Surgery, Faculty of Medicine, Ondokuz Mayis University, Samsun, Turkey

ARTICLE INFO

Keywords:
Parathyroid adenoma
Magnetic resonance imaging
Diagnostic performance
Ultrasonography
99mTc-Sestamibi

ABSTRACT

Purpose: The aim of this study was to assess the feasibility of four-dimensional magnetic resonance imaging (4D MRI) at 3 T for the localization of parathyroid adenomas.

Materials and Methods: Preoperative 4D MRI scans, encompassing dynamic contrast-enhanced (DCE) sequences and non-contrast enhanced (non-CE) sequences, including a T2-weighted multipoint Dixon (T2-mDixon) sequence, with in-phase, out-phase, and water-only images, were evaluated retrospectively in 41 patients with surgically proven parathyroid lesions. Two readers who were blinded to the surgical findings independently reviewed the images in two sessions (non-CE sequences alone and non-CE + DCE sequences). The MRI localization of the suspected adenoma in each session and the consensus interpretation of the MRI images, were compared with the surgical results and interobserver agreement was assessed.

Results: By interpreting the non-CE sequences alone, reader 1 correctly localized 34 parathyroid lesions (sensitivity 81.0%, positive predictive value (PPV) 87.2%), and reader 2 correctly localized 34 parathyroid lesions (sensitivity 81.0%, PPV 91.9%). With the addition of DCE sequences, reader 1 correctly identified 35 parathyroid lesions (sensitivity 83.3%, PPV 87.5%), while reader 2 correctly identified 36 parathyroid lesions (sensitivity 85.7%, PPV 92.3%). Overall, MRI detected 38 parathyroid lesions (sensitivity 90.5%, PPV 95.0%). Interobserver agreement was slightly superior in non-CE + DCE sequences compared to non-CE sequences alone ($\kappa = 0.796$ vs. $\kappa = 0.738$).

Conclusion: 4D MRI with DCE sequencing is a reliable method for the localization of parathyroid adenomas.

1. Introduction

Primary hyperparathyroidism (PHPT) is a clinical condition characterized by increased serum calcium (Ca) and parathyroid hormone (PTH) levels. Most often, the etiology is a single parathyroid adenoma; however, multiple glandular hyperplasia or multiple adenomas may rarely be the underlying causes [1,2]. Surgery offers a curative treatment for PHPT, so preoperative localization with imaging is important in order to reduce surgical time, incision, and related complications [3]. Imaging techniques are based on the hypervascular nature of the enlarged gland. In ultrasound (US), the gland has a hypoechoic appearance with a characteristic feeding artery sign [4,5]. In Technetium-99 m (99mTc) sestamibi scintigraphy, sestamibi accumulates in the mitochondria of the hypermetabolic gland. In computed tomography (CT) and magnetic resonance imaging (MRI), parathyroid adenomas appear as hyperenhancing lesions during early arterial phases [6–11].

US and 99mTc-sestamibi are the two first-line imaging techniques for the preoperative localization of parathyroid lesions. They are complementary to each other, and the combined use of US and 99mTc-sestamibi is reported to have a high sensitivity, up to 93.4%. [6,12–14]. If the setting of US or 99mTc-sestamibi fails to localize the parathyroid lesions, these two techniques reveal discrepant findings, or the PHPT is recurrent or persistent after surgery, CT and MRI are considered as second-line imaging modalities [15,16]. In some cases, accompanying thyroid disease or the need to evaluate neck anatomy better may necessitate the use of cross-sectional imaging modalities. Recently, four-dimensional imaging protocols were defined for both CT (4D CT) and MRI (4D MRI) [6,8–11,17]. In these techniques, the 'fourth dimension' is the time-resolved enhancement kinetics of the lesion, which serves as functional information. The ability to image the entire anatomy, including possible ectopic locations, and the combination of anatomical information with functional information from dynamic contrast-

* Corresponding author at: Ondokuz Mayis University, Faculty of Medicine, Department of Radiology, 55139 Kurupelit, Samsun, Turkey.
E-mail address: dr.mesutozturk@gmail.com (M. Ozturk).

https://doi.org/10.1016/j.ejrad.2019.01.022
Received 3 August 2018; Received in revised form 3 November 2018; Accepted 21 January 2019

enhanced (DCE) images make CT and MRI valuable imaging modalities for the preoperative localization of hyperfunctioning parathyroid glands.

The sensitivity of MRI at 1.5 T scanners has been reported at approximately 80% [18–21]. After 3 T magnets were introduced into clinical practice, an increment in the signal-to-noise and contrast-to-noise ratio and excellent fat saturation, thanks to chemical shift-based, water-fat separation techniques, yielded improved image quality and lesion detectability. Parathyroid adenomas exhibit a hypervascular nature on MRI also, but some studies reported only a moderate contribution of time-resolved enhancement kinetics to diagnosis [7,9,10].

The aim of the present study was to assess the diagnostic value of 4D MRI at 3 T in the localization of parathyroid lesions, with respect to the surgical data, and to assess the contribution of DCE images to the diagnosis.

2. Materials and methods

2.1. Patients

This retrospective study was approved by our institutional ethics committee, and the requirement for informed consent was waived, owing the nature of the study. A retrospective search of our hospital database revealed 51 patients who underwent MRI examination at 3 T for a preliminary diagnosis of PHPT between December 2016 and April 2018. The inclusion criteria were: high serum Ca level (reference: 8.5–10 mg/dl), high serum PTH level (reference PTH: 15–65 pg/ml), and surgically removed parathyroid lesion. Eight patients without pathological results were excluded, as were two patients because of severe motion artifacts on MRI. All patients had US and 99mTc-sestamibi results available.

2.2. 4D MRI technique

MRI examinations of the patients were performed with a 3 T MR system (Ingenia, Philips Healthcare, Netherlands). Patients were positioned supine, and a dedicated neck coil was used. The field of view was set to include the area spanning from the angle of the mandible to the level of the carina. The standard MRI protocol for a preliminary diagnosis of PHPT in our center includes the following sequences: a three-plan localizer; an axial turbo-spin echo T2-weighted multipoint Dixon TSE sequence (T2-mDixon), with in-phase, out-phase and water only images; an axial T1-weighted TSE sequence; a sagittal T1-weighted TSE sequence; a coronal short tau inversion recovery (STIR) sequence; an axial fat-suppressed, dynamic contrast-enhanced (DCE) T1-weighted 3D radial gradient-recalled echo sequence (volumetric interpolated breath-hold examination (VIBE)). The DCE sequence consisted of one pre-contrast and eight post-contrast images with a temporal resolution of 15 s. After the acquisition of the pre-contrast image, an intravenous bolus of 0.1 mmol/kg of a gadolinium-based contrast agent was injected, with a flow rate of 2 ml/s, followed by 20 ml of saline flush, using an automatic injector. The post-contrast scans started after the visualization of aortic arch enhancement through a real time MRI monitoring of the contrast bolus. After the image acquisition, subtracted images were constructed by subtracting the pre-contrast images from the post-contrast ones on a pixel-by-pixel basis. The MRI protocol and imaging parameters are displayed in Table 1.

2.3. Image interpretation

Two radiologists (reader 1: A.V.P., nine years of experience in head and neck imaging; reader 2: M.E., 10 years of experience in head and neck imaging), who were both blinded to the surgical, pathological, and other imaging modality results of the patients, reviewed the MRI studies independently in two sessions. First, the radiologists evaluated the non-contrast enhanced (non-CE) sequences alone (the sequences other than the axial 3D VIBE); second, they examined the non-CE sequences with the addition of the DCE sequence (axial 3D VIBE). The second session was immediately after the first one, without an interval in which the progressive contribution of the DCE sequence to the non-CE sequences could be assessed. Each reader evaluated the images for the localization of the suspected lesion in its quadrant (right or left with respect to the midline; upper or lower with respect to the transverse line at the middle of the thyroid gland).

The non-CE sequences session was primarily based on the evaluation of the T2-mDixon sequence. The radiologists used other sequences if necessary. The following features were used in the image evaluation: hyperintense appearance compared to the thyroid gland in the T2-mDixon water-only images, presence of a hypointense cleavage plane between the lesion and thyroid gland in T2-mDixon out-phase images, rapid arterial enhancement, and wash-out on DCE images [11]. Rapid arterial enhancement was defined as vivid enhancement of the suspected lesion compared to thyroid parenchyma on the first or second post-contrast phases, and wash-out was defined as a loss of contrast on the delayed phases, which were based on visual assessment (Fig. 1). In case of doubt about the enhancement pattern, the radiologists drew a region of interest on the lesion and measured signal intensity in consecutive phases. The readers rated the DCE images for their contribution to non-CE sequences to diagnose a parathyroid lesion (1 = the lesion was not visible on DCE images, 2 = the lesion was visible on DCE but did not contribute to non-CE sequences, 3 = moderate contribution to non-CE sequences, 4 = very helpful and increased confidence in the diagnosis). The two readers then compared their discrepant results and reached a final consensus.

2.4. US and 99mTc-sestamibi examinations

US and 99mTc-sestamibi examination reports for all patients were available in the hospital database, and quadrant localizations were defined with respect to midline and transverse line through the thyroid gland, as previously described in the setting of patient care. US examinations of the patients were performed using the Siemens ACUSON S2000 US system (Siemens Medical Solutions, Mountain View, CA, USA). The examination covered the area from the upper border of the thyroid cartilage to the sternal notch in both transverse and longitudinal planes. A parathyroid lesion was considered if a characteristic hypoechoic lesion with/without a polar vessel sign was detected [5]. Both early and delayed-phase post-infusion images were obtained for 99-mTc-sestamibi scans, and delayed imaging with single emission computed tomography (SPECT) was also obtained from every patient. Residual uptake of the radioactive agent on the delayed phase was accepted as positive for a parathyroid lesion.

2.5. Surgical treatment and histopathological results

Surgery of the patients was performed by a surgeon (C.P.) with 22 years of experience in parathyroid and thyroid surgery. The operation technique was either parathyroidectomy or open bilateral neck exploration, depending on the preoperative imaging results or the presence of concomitant thyroid disease. The surgery was deemed to be successful and terminated if the removed lesion was diagnosed as a hypercellular parathyroid gland on the frozen section reading and the serum PTH level decreased by more than 50% of the basal level of the preoperative setting. Final diagnosis was based on the histopathological examination.

2.6. Statistical analysis

Statistical analysis was performed with the Statistical Package for Social Sciences 15.0 (SPSS, Inc., Chicago, IL, USA) for Windows. A p value less than 0.05 was accepted as statistically significant. Categorical variables were expressed in frequency, and continuous variables were

Table 1
The scan parameters of a dedicated MRI protocol for patients with primary hyperparathyroidism.

Sequence	TR/TE (ms)	FOV (cm × cm)	Matrix	Slice thickness (mm)	Acquisition time (min)
Axial T2-mDixon TSE	3422/100	200 × 200	288 × 219	3.5	04:13
Axial T1 TSE	531/7	200 × 200	288 × 219	3.5	03:40
Sagittal T1 TSE	561/16	200 × 220	332 × 288	4	01:49
Coronal STIR	2484/60	200 × 220	200 × 168	3.5	02:42
Axial 3D VIBE	3.5/1.6	250 × 200	168 × 133	3	02:25

TR / TE: Repetition time / Echo time, FOV: field of view, mDixon: multipoint Dixon, TSE: turbo spin echo, STIR: short tau inversion recovery, VIBE: volumetric interpolated breath-hold examination.

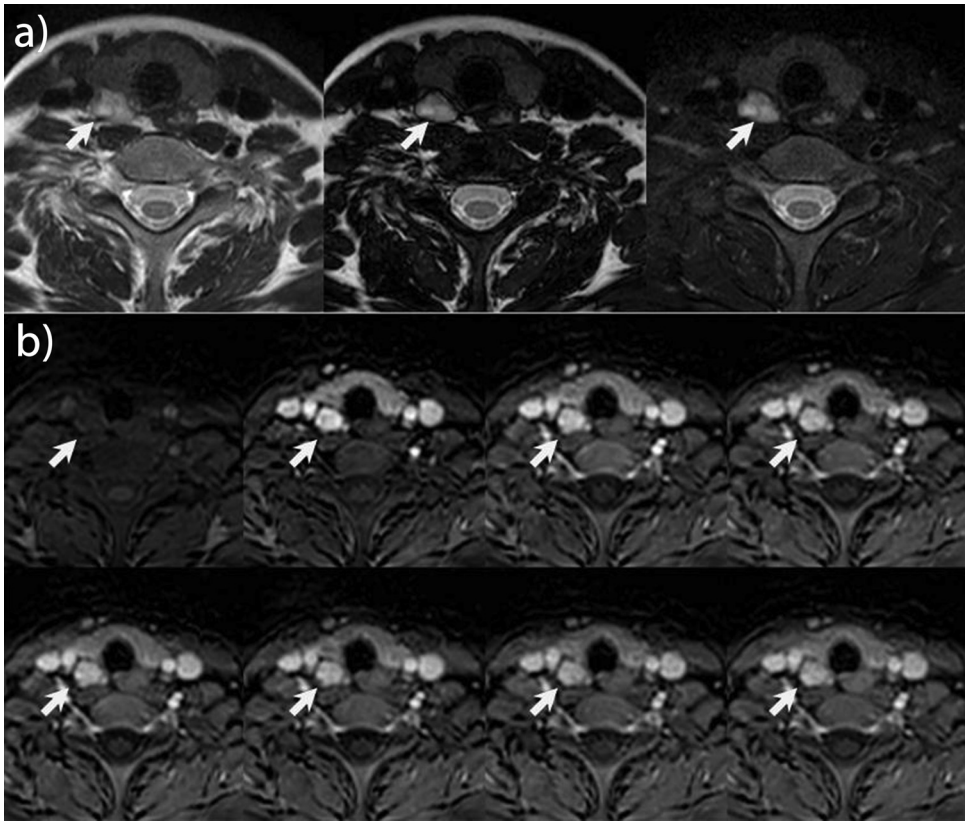

Fig. 1. MR images of 28-year-old woman with primary hyperparathyroidism. a) Axial T2-mDixon sequence with in-phase, out-phase, and water-only images show a hyperintense lesion (arrows) located in the right lower quadrant. A thin cleavage plane from the thyroid gland is seen on the out-phase image. b) Axial fat-suppressed T1-weighted contrast-enhanced images show strong and early arterial enhancement of the lesion (arrows).

presented as mean ± standard deviation (SD). The diagnostic performances of each MRI interpretation were assessed with diagnostic accuracy measures by comparing the MRI interpretations with surgical and histopathological results as the gold standard. A correctly identified quadrant of the lesion was used to assess accuracy. Sensitivity and positive predictive values (PPV) were calculated for each interpretation and imaging modality. McNemar's test was used to compare image interpretations. Agreement between the readers' interpretations was assessed using Cohen's kappa coefficient (κ), whereby the strength of agreement was accepted as poor if $\kappa < 0$ (less than expected by chance), slight if $\kappa = 0.01–0.20$, fair if $\kappa = 0.21–0.40$, moderate if $\kappa = 0.41–0.60$, substantial if $\kappa = 0.61–0.80$, and almost perfect if $\kappa = 0.81–1.00$ [22].

3. Results

3.1. Patients

Forty-one patients were enrolled in the study (34 women and seven men). The mean age of the study population was 50.37 ± 10.63 years (range: 28–72). The mean preoperative serum Ca level was 11.3 ± 0.77 mg/dl (range: 10.3–13.2), and the mean preoperative serum PTH level was 164.99 ± 69.4 pg/dl (range: 74–420). The mean time interval between MRI examination and surgery was 68.5 days (range: 3–361).

3.2. Surgery and pathology results

According to the surgical results, 42 parathyroid lesions were diagnosed in 41 patients. Forty patients were diagnosed with a single adenoma, and one patient was diagnosed with hyperplasia of two parathyroid glands. Four lesions were located at the right upper quadrant, 15 lesions at the right lower quadrant, four lesions at the left upper quadrant, and 19 lesions at the left lower quadrant.

3.3. MRI interpretations of readers

In the non-CE sequences interpretation session, reader 1 correctly localized 34 parathyroid lesions (sensitivity 81.0% and PPV 87.2%). With the addition of DCE sequences, he localized 35 lesions (sensitivity 83.3%, PPV 87.5%). Reader 2 diagnosed 34 parathyroid lesions in the non-CE sequences session (sensitivity 81.0% and PPV 91.9%), but was able to localize 36 parathyroid lesions in the non-CE plus DCE sequences session (sensitivity 85.7% and PPV 92.3%). For both readers, the addition of DCE sequences increased sensitivity and PPV, although the difference was not found to be statistically significant (p = 1.000

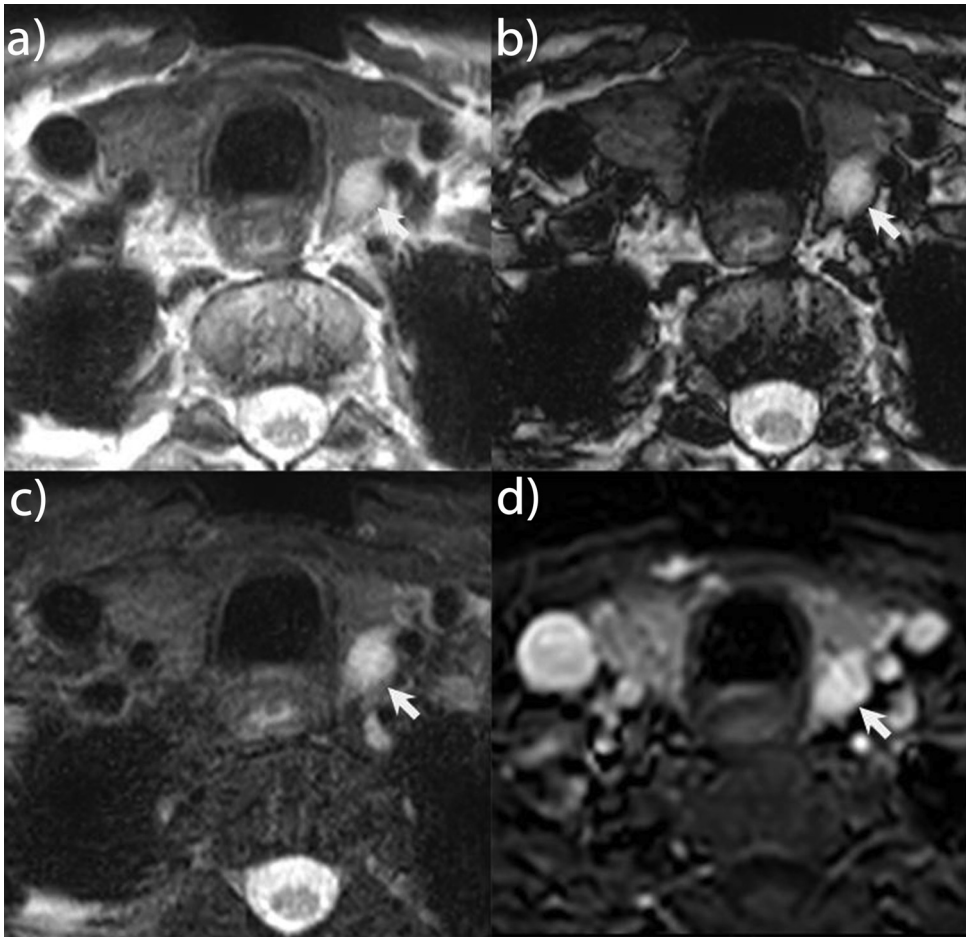

Fig. 2. MR images of a 59-year-old man with primary hyperparathyroidism. Axial T2-mDixon in-phase (a), out-phase (b), and water-only (c) images show an oval hyperintense lesion (arrows) posterior to the left lobe of the thyroid gland. The lesion (arrow) demonstrates strong enhancement in the arterial phase (d). The lesion was diagnosed as a papillary thyroid carcinoma.

and p = 0.500, respectively). Interobserver agreement was slightly superior in the non-CE plus DCE sequences session (κ = 0.796 vs. κ = 0.738).

3.4. Overall diagnostic performance of 4D MRI and lesion characteristics

With consensus agreement, 4D MRI correctly localized 38 parathyroid lesions (sensitivity 90.5% and PPV 95%). There were four false-negative results, in which MRI was unable to localize parathyroid lesions. In two cases, MRI made a wrong localization. One of these lesions was diagnosed as a malignant thyroid nodule (Fig. 2).

The average lesion size was 12.7 × 8.2 mm (range 2–23). Thirty-one lesions (81.6%) were hyperintense, and seven lesions (18.4%) were isointense compared to the thyroid gland on the T2-mDixon sequence. In thirty-two lesions (84.2%), there was a cleavage plane between the lesion and thyroid gland, which helped to differentiate it from thyroid tissue. The average score of the DCE images to lesion localization was 2.6. Four lesions (10.5%) were not visible on the DCE images, while 10 lesions (26.3%) were visible but did not contribute to non-CE sequences (Fig. 3). The DCE images made a moderate contribution to lesion localization in 21 cases (55.3%). In three lesions (7.8%), the DCE images was very helpful and made a significant contribution to the localization of parathyroid lesions. An arterial-phase higher enhancement of a parathyroid lesion was observed in 26 lesions (68.4%), and wash-out of contrast was observed in 16 (42.1%) lesions.

3.5. US and 99mTc-sestamibi results

The sensitivity and PPV of US were 76.2% (32/42) and 100% (32/32), respectively. 99mTc-sestamibi had 71.4% (30/42) sensitivity and 96.8% (30/31) PPV. When US and 99mTc-sestamibi were combined, sensitivity and PPV values were found to be 90.5% and 97.4%, respectively. US correctly localized six lesions missed by 99mTc-sestamibi, and 99mTc-sestamibi correctly localized six lesions missed by US. In the case of one lesion, US and 99mTc-sestamibi indicated different sides (right lower vs. left lower), but the parathyroid lesion was found on the side indicated by US.

3.6. Consistent and discrepant findings between US, 99mTc-sestamibi, and MRI

US and 99mTc-sestamibi results were consistent with the surgical findings in 25 lesions. Of these cases, MRI correctly localized all except one (24/25) lesion, in the same quadrant as US and 99mTc-sestamibi. In 12 lesions, US or 99mTc-sestamibi was negative for lesion detection, and MRI localized all lesions missed by US and four lesions missed by 99mTc-sestamibi. In the case of one lesion, US and 99mTc-sestamibi indicated different sides, and MRI localized the lesion on the side that 99mTc-sestamibi indicated; however, that lesion was diagnosed as a malignant thyroid nodule, and the parathyroid lesion was detected on the quadrant indicated by US. In four lesions, both US and 99mTc-sestamibi revealed a negative scan for parathyroid lesions, but MRI was able to localize all of these lesions (Fig. 4). In the setting in which US

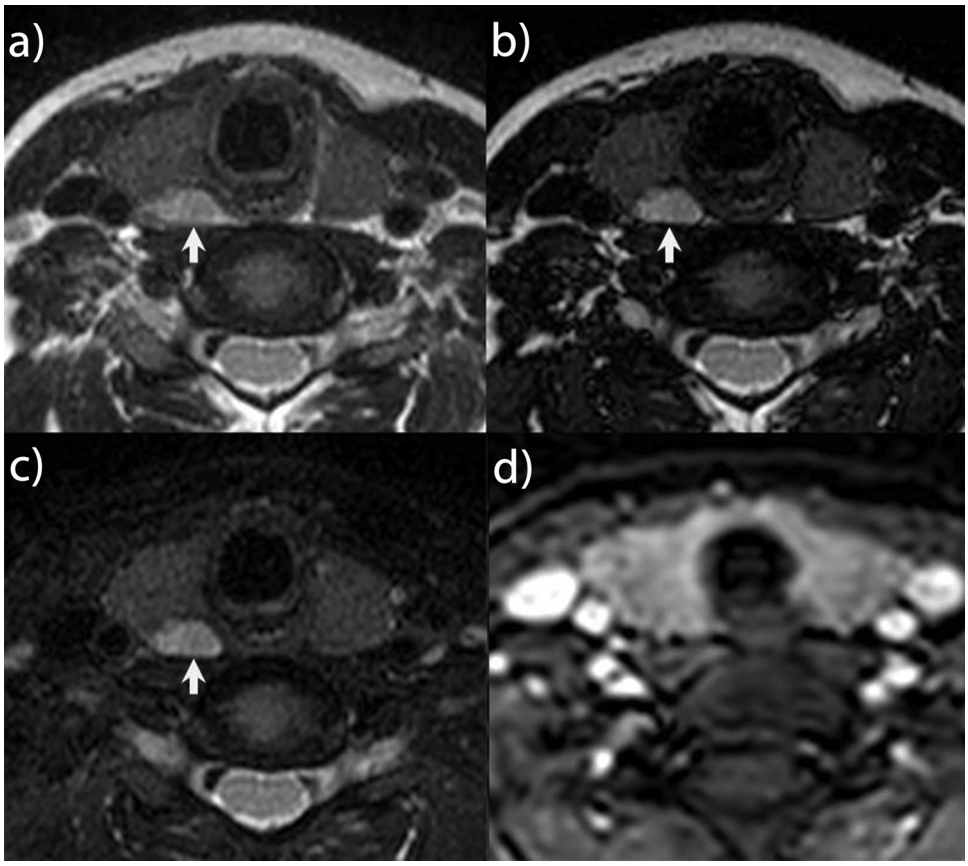

Fig. 3. MR images of a 33-year-old woman with primary hyperparathyroidism. Axial T2-mDixon in-phase (a), out-phase (b), and water-only (c) images show an oval hyperintense lesion (arrows) posterior to the right lobe of the thyroid gland. The lesion cannot be distinguished from the thyroid gland on the contrast-enhanced T1-weighted images (d). Pathological examination revealed a parathyroid adenoma.

and 99mTc-sestamibi revealed discrepant results or both modalities failed to localize the parathyroid lesions, MRI was able to localize 14/17 lesions correctly (sensitivity 82.4%, PPV 93.3%). The sensitivity and PPV of combined US and MRI, 99mTc-sestamibi and MRI, and US, MRI and 99mTc-sestamibi are displayed in Table 2.

4. Discussion

The study results confirmed that 4D MRI is a feasible modality for the localization of parathyroid lesions. Data analysis demonstrated that MRI had higher sensitivity (90.5%) compared to US (76.2%) and 99mTc-sestamibi (71.4%). Furthermore, the sensitivity of MRI alone was equivalent to the sensitivity of combined use of US and 99mTc-sestamibi. Combined use of MRI with US or 99mTc-sestamibi yielded higher sensitivity than individual use of these techniques, which suggests that MRI may also be an important complementary preoperative imaging modality. Combined US, 99mTc-sestamibi, and MRI revealed a sensitivity of 100%.

US and 99mTc-sestamibi are the two first-line imaging modalities for the localization of parathyroid lesions [12,13]. The sensitivity of US and 99mTc-sestamibi in the localization of parathyroid lesions have been reported to be approximately 90% [6,23]. Major disadvantages of US are user-dependency, low image quality owing to patient habitus or obesity, and failure to demonstrate ectopic glands such as the mediastinum. Although there was one mediastinal parathyroid lesion in our study, the sensitivity of US was 76.2%. However, our study population was PHPT patients whose MRI examinations were available; thus, the overall diagnostic performance of US may be higher because of the cases in which MRI was not needed. On the other hand, 99mTc-sestamibi has some disadvantages, such as lower spatial resolution and exposure to ionizing radiation. 99mTc-sestamibi may not localize all glands in multiglandular disease and may reveal false-positive results in the setting of accompanying malignant thyroid nodules [24,25]. In our study, there was one patient with hyperplasia of two parathyroid glands, and 99mTc-sestamibi failed to identify one of the two affected glands. Additionally, there was one false-positive lesion, in which one malignant thyroid nodule was incorrectly reported as a parathyroid adenoma.

In cases of inconclusive first-line imaging results, persistent or recurrent hyperparathyroidism, or a history of previous surgery, CT and MRI are used as second-line imaging techniques. These cross-sectional imaging modalities have the advantage of imaging the entire anatomy, including possible ectopic localizations such as the upper mediastinum. Since 4D CT was introduced in 2006, it has been reported to have high sensitivity for the localization of parathyroid lesions [17]. The hypervascular nature of parathyroid lesions on CT has prompted the question whether this feature could be used in MRI. MRI also has the advantages of high soft-tissue resolution and no radiation exposure. Recent studies confirmed the hypervascular nature of parathyroid lesions seen in MRI, but the contribution of this feature to lesion localization is still worth researching [7,9,10].

4D MRI is obtained by combining the anatomical information from the non-CE sequences with the functional information from the DCE images. The ‘fourth dimension’ is the time-dependent enhancement kinetics of the lesion [9,10,17]. Recent literature has demonstrated that parathyroid adenomas show rapid arterial enhancement after bolus-injection of gadolinium-based contrast agents, as demonstrated on CT [9,10]. However, some authors reported that this feature contributed only moderately to the diagnosis [6,7]. Although rapid arterial enhancement on MRI was not found to be particularly helpful in the diagnosis, it was shown to increase diagnostic confidence [6,7]. In the present study, the value of DCE imaging to non-CE sequences was assessed by performing image evaluation in two sessions and by rating the DCE sequences for their contribution to non-CE sequences. For both readers, the DCE sequences increased the detectability of lesions, but not by a statistically significant amount. However, DCE sequences

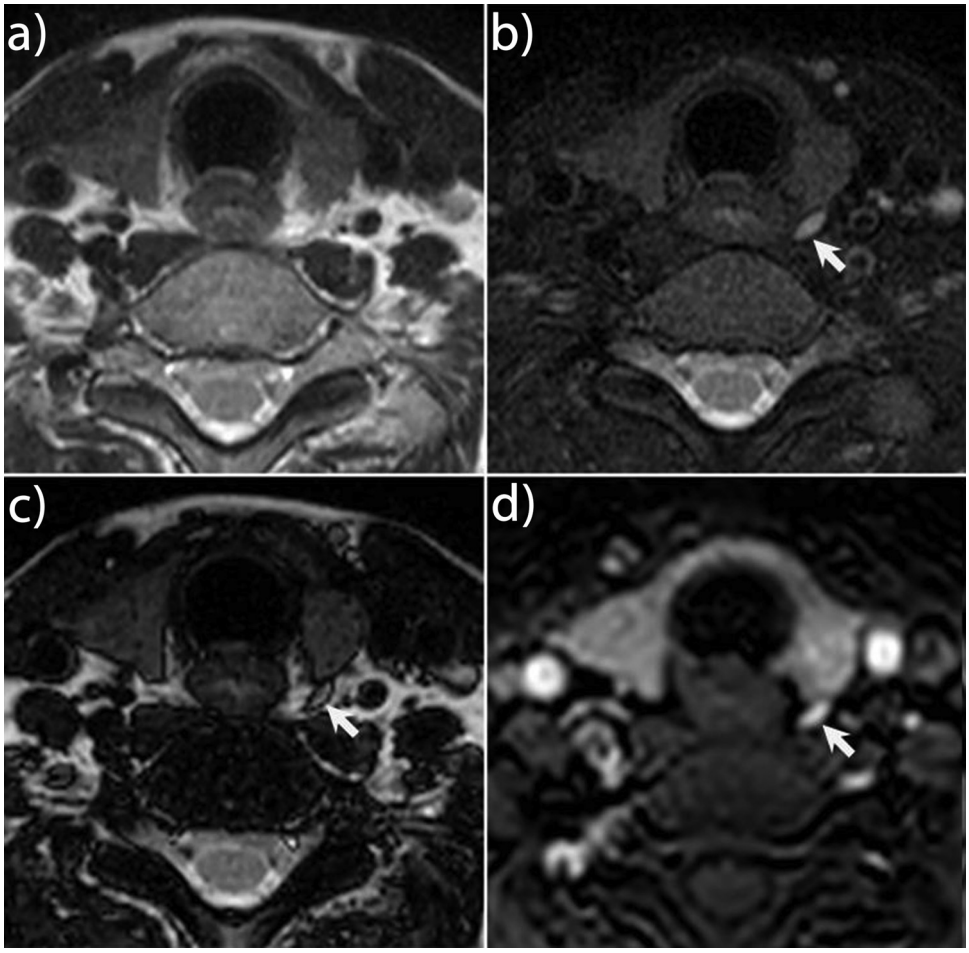

Fig. 4. MR images of a 46-year-old man with primary hyperparathyroidism. US and 99mTc-sestamibi revealed negative results for a parathyroid lesion. Axial T2-mDixon in-phase image (a) is negative for a parathyroid lesion. T2-mDixon water-only (b), and out-phase (c) images demonstrate an oval lesion (arrows) located posterior to the left thyroid gland. The lesion (arrow) demonstrates strong enhancement in the arterial phase (d). The lesion was diagnosed as a parathyroid adenoma.

Table 2
The sensitivity and positive predictive values of US, 99mTc-sestamibi, MRI, and combined modalities for the localization of parathyroid lesions.

Imaging Modality	Sensitivity % (n)	PPV % (n)
US	76.2 (32/42)	100 (32/32)
99mTc-sestamibi	71.4 (30/42)	96.8 (30/31)
MRI	90.5 (38/42)	95.0 (38/40)
US + 99mTc-sestamibi	90.5 (38/42)	97.4 (38/39)
US + MRI	95.2 (40/42)	95.2 (40/42)
99mTc-sestamibi + MRI	97.6 (41/42)	97.6 (41/42)
US + 99mTc-sestamibi + MRI	100 (42/42)	95.5 (42/44)

US: ultrasound, MRI: magnetic resonance imaging, PPV: positive predictive value.

contributed to the diagnosis in 24 cases. Four lesions were not visible on DCE, while 10 lesions were visible but did not contribute to the diagnosis. These results suggest that even non-CE MRI at 3 T may be used for parathyroid lesion detection, and a contrast agent may be selectively used for cases with undetermined results.

There are limited data about the use of 3 T MRI for the localization of parathyroid lesions, but studies have reported the high sensitivity of MRI for lesion localization [6,7,9–11]. Argiro et al. reported the sensitivity of MRI as 97.8% [6]. In their study, MRI had higher sensitivity than US (89.1%) and 99mTc-sestamibi (83.6%), even when the latter were combined (93.4%). Grayev et al. reported a lower sensitivity of MRI (64%) than US (88%) and 99mTc-sestamibi (72%), but combined use of MRI and 99mTc-sestamibi yielded 88% sensitivity [7]. Both studies found that DCE sequencing was not greatly helpful to lesion detection, although it was crucial in a limited number of cases. Similarly, Sacconi et al. reported moderate usefulness of DCE images for the diagnosis of parathyroid adenomas [11]. Results from the present study also confirmed that DCE images were not greatly helpful for diagnosis but moderately increased the diagnostic confidence. This finding may be explained by the superiority of high soft-tissue contrast of MRI to early arterial contrast enhancement. A high signal on T2-mDixon images and presence of Indian ink artifact between the lesion and thyroid tissue are well-known features of parathyroid adenomas, and most of the lesions in the present study demonstrated these features [11].

In this study, four lesions could not be localized by US or 99mTc-sestamibi but were correctly localized by MRI. When these two techniques revealed negative or discrepant results, MRI was able to localize 14/17 lesions correctly (sensitivity 82.4%, PPV 93.3%). Combined use of MRI with US or 99mTc-sestamibi demonstrated higher sensitivity (95.2% and 97.6%) than US or 99mTc-sestamibi alone (76.2% and 71.4%) or in combination (90.5%). However, in cases in which US and 99mTc-sestamibi localized the same quadrant, MRI was also consistent with US and 99mTc-sestamibi results. These findings confirmed that MRI was a complementary imaging modality and are in agreement with previous authors who found that MRI was a second-line imaging modality in cases in which US and 99mTc-sestamibi revealed discrepant or inconclusive results.

This study has some limitations. First, it was a retrospective study. Second, the number of patients was limited. More studies with larger

populations are needed to validate these findings. Third, there was no control group, and all patients in the study population were known to have PHPT. However, the interpreters were blinded to other imaging modality and surgery results.

5. Conclusion

The results of this study demonstrated that 4D MRI is a feasible modality in the localization of parathyroid lesions. MRI was a useful complementary imaging modality in cases in which first-line imaging techniques revealed negative or discrepant results. With its high soft-tissue resolution and the advantages of water-fat separation techniques, MRI was able to identify parathyroid lesions, even in non-CE sequences. Although it was not found statistically significant, the addition of DCE images to non-CE images improved lesion detection. However, DCE images showed moderate improvement in the diagnostic confidence.

Funding

This research did not receive any specific grant from funding agencies in the public, commercial, or not-for-profit sectors.

Conflict of interest

None.

References

[1] D.M. Press, A.E. Siperstein, E. Berber, J.J. Shin, R. Metzger, J. Jin, et al., The prevalence of undiagnosed and unrecognized primary hyperparathyroidism: a population-based analysis from the electronic medical record, Surgery 154 (2013) 1232–1238.
[2] B. Abboud, G. Sleilaty, E. Helou, E. Mansour, C. Tohme, R. Noun, et al., Existence and anatomic distribution of double parathyroid adenoma, Laryngoscope 115 (2005) 1128–1131.
[3] M. Barczyński, S. Cichoń, A. Konturek, W. Cichoń, Minimally invasive video-assisted parathyroidectomy versus open minimally invasive parathyroidectomy for a solitary parathyroid adenoma: a prospective, randomized, blinded trial, World J. Surg. Oncol. 30 (2006) 721–731.
[4] S. Rickes, J. Sitzy, H. Neye, K.W. Ocran, W. Wermke, High-resolution ultrasound in combination with colour-Doppler sonography for preoperative localization of parathyroid adenomas in patients with primary hyperparathyroidism, Ultraschall Med. 24 (2003) 85–89.
[5] S.B. Reeder, T.S. Desser, R.J. Weigel, R.B. Jeffrey, Sonography in primary hyperparathyroidism: review with emphasis on scanning technique, J. Ultrasound Med. 21 (2002) 539–552.
[6] R. Argirò, D. Diacinti, B. Sacconi, A. Iannarelli, D. Diacinti, C. Cipriani, et al., Diagnostic accuracy of 3T magnetic resonance imaging in the preoperative localisation of parathyroid adenomas: comparison with ultrasound and 99mTc-sestamibi scans, Eur. Radiol. 28 (2018) 4900–4908.
[7] A.M. Grayev, L.R. Gentry, M.J. Hartman, H. Chen, S.B. Perlman, S.B. Reeder, Presurgical localization of parathyroid adenomas with magnetic resonance imaging at 3.0 T: an adjunct method to supplement traditional imaging, Ann. Surg. Oncol. 19 (2012) 981–989.
[8] A.K. Lundstroem, W. Trolle, C.H. Soerensen, P.S. Myschetzky, Preoperative localization of hyperfunctioning parathyroid glands with 4D-CT, Eur. Arch. Otorhinolaryngol. Suppl. 273 (2016) 1253–1259.
[9] S. Merchavy, J. Luckman, M. Guindy, Y. Segev, A. Khafif, 4D MRI for the localization of parathyroid adenoma: a novel method in evolution, Otolaryngol. Head. Neck Surg. 154 (2016) 446–448.
[10] K. Nael, J. Hur, A. Bauer, R. Khan, A. Sepahdari, R. Inampudi, et al., Dynamic 4D MRI for characterization of parathyroid adenomas: multiparametric analysis, AJNR Am. J. Neuroradiol. 36 (2015) 2147–2152.
[11] B. Sacconi, R. Argirò, D. Diacinti, A. Iannarelli, M. Bezzi, C. Cipriani, et al., MR appearance of parathyroid adenomas at 3 T in patients with primary hyperparathyroidism: what radiologists need to know for pre-operative localization, Eur. Radiol. 26 (2016) 664–673.
[12] N.A. Johnson, M.E. Tublin, J.B. Ogilvie, Parathyroid imaging: technique and role in the preoperative evaluation of primary hyperparathyroidism, AJR Am. J. Roentgenol. 188 (2007) 1706–1715.
[13] C.D. Phillips, D.R. Shatzkes, Imaging of the parathyroid glands, Semin. Ultrasound CT MR 33 (2012) 123–129.
[14] J.W. Kunstman, J.D. Kirsch, A. Mahajan, R. Udelsman, Parathyroid localization and implications for clinical management, J. Clin. Endocrinol. Metab. 98 (2013) 902–912.
[15] A. van Dalen, C.P. Smit, T.J. van Vroonhoven, H. Burger, E.E. de Lange, Minimally invasive surgery for solitary parathyroid adenomas in patients with primary hyperparathyroidism: role of US with supplemental CT, Radiology 220 (2001) 631–639.
[16] F. Lumachi, A. Tregnaghi, P. Zucchetta, M.C. Marzola, D. Cecchin, P. Marchesi, et al., Technetium-99m sestamibi scintigraphy and helical CT together in patients with primary hyperparathyroidism: a prospective clinical study, Br. J. Radiol. 77 (2004) 100–103.
[17] S.E. Rodgers, G.J. Hunter, L.M. Hamberg, D. Schellingerhout, D.B. Doherty, G.D. Ayers, Improved preoperative planning for directed parathyroidectomy with 4-dimensional computed tomography, Surgery 140 (2006) 932–941.
[18] M.B. Gotway, C.B. Higgins, MR imaging of the thyroid and parathyroid glands, Magn. Reson. Imaging Clin. N. Am. 8 (2000) 163–182.
[19] E.L. HÄnninen, T.J. Vogl, T. SteinmÜller, J. Ricke, P. Neuhaus, R. Felix, Preoperative contrast-enhanced MRI of the parathyroid glands in hyperparathyroidism, Invest. Radiol. 35 (2000) 426–430.
[20] M.B. Gotway, G.P. Reddy, W.R. Webb, E.T. Morita, O.H. Clark, C.B. Higgins, Comparison between MR imaging and 99mTc MIBI scintigraphy in the evaluation of recurrent or persistent hyperparathyroidism, Radiology 218 (2001) 783–790.
[21] J.E. Kabala, Computed tomography and magnetic resonance imaging in diseases of the thyroid and parathyroid, Eur. J. Radiol. 66 (2008) 480–492.
[22] J.R. Landis, G.G. Koch, The measurement of observer agreement for categorical data, Biometrics (1977) 159–174.
[23] K.J. Nichols, M.B. Tomas, G.G. Tronco, J.N. Rini, B.D. Kunjummen, K.S. Heller, et al., Preoperative parathyroid scintigraphic lesion localization: accuracy of various types of readings, Radiology 248 (2008) 221–232.
[24] S.L. Sugg, E.A. Krzywda, M.J. Demeure, S.D. Wilson, Detection of multiple gland primary hyperparathyroidism in the era of minimally invasive parathyroidectomy, Surgery 136 (2004) 1303–1309.
[25] W.P. Kluijfhout, W.M. Vorselaars, M.R. Vriens, I.H.B. Rinkes, G.D. Valk, B. Keizer, Enabling minimal invasive parathyroidectomy for patients with primary hyperparathyroidism using Tc-99m-sestamibi SPECT–CT, ultrasound and first results of 18F-fluorocholine PET–CT, Eur. J. Radiol. 84 (2015) 1745–1751.